engineering proceedings

MDPI

Proceeding Paper

Combining Additive Manufacturing Techniques for High-Performance Stiffened Panels †

Alberto Pedreira, Adrián Rodríguez, Noelia González-Castro, Beatriz Simoes-Pereira and Pablo Romero-Rodriguez *

AIMEN Technology Centre, Relva 27A-O Porriño, 36410 Pontevedra, Spain; alberto.pedreira@aimen.es (A.P.); adrian.rvazquez@aimen.es (A.R.); noelia.gonzalez@aimen.es (N.G.-C.); beatriz.simoes@aimen.es (B.S.-P.)

* Correspondence: pablo.rodriguez@aimen.es

† Presented at the 14th EASN International Conference on "Innovation in Aviation & Space towards sustainability today & tomorrow", Thessaloniki, Greece, 8–11 October 2024.

Abstract: The additive manufacturing of high-performance thermoplastics, including high-temperature materials and continuous fiber reinforcement, are extensively being developed worldwide. In this work, we combined laser-assisted in situ consolidation tape laying and fused filament fabrication to manufacture a 100% thermoplastic stiffened panel in three stages with innovative designs using LMPAEK-PEKK carbon fiber-reinforced polymers. The overprinting of gyroid structures on top of ATL laminates assisted by lasers have shown very good adhesion. Mechanical characterization by flatwise and four-point bending tests have shown tensile strength in the range of 10 MPa (flatwise) and 889 MPa (four-point bending). Tomography analysis shows the optimization roadmap to enhance mechanical properties by improving temperature management during manufacturing.

Keywords: additive manufacturing; laser-assisted in situ consolidation; automated tape laying; fused filament fabrication; gyroid stiffeners; flatwise; four-point bending test

Academic Editors: Spiros Pantelakis, Andreas Strohmayer and Nikolaos Michailidis

Published: 18 March 2025

Citation: Pedreira, A.; Rodríguez, A.; González-Castro, N.; Simoes-Pereira, B.; Romero-Rodriguez, P. Combining Additive Manufacturing Techniques for High-Performance Stiffened Panels. *Eng. Proc.* **2025**, *90*, 59. https://doi.org/10.3390/engproc2025090059

1. Introduction

Additive manufacturing is envisaged to revolutionize the composite structures' value chains by widening their design space, lightweight potential, and deployment of multifunctional materials which are reversibly processed, enabling disassembly, multifunctionality, and repair [1–3]. Among all AM techniques for high-performance composite structures, the aviation sector looks closely to automated tape laying and fused filament fabrication techniques due to their ability to produce structural parts with commercially available materials [4]. However, there is the need for a more systematic optimization process based on data, as well as controlling the manufacturing parameters along the whole process, which is an intrinsic challenge for this kind of out-of-mold manufacturing processes [5]. In this work within the DOMMINIO Project, we present the combination of the laser-assisted automated in situ consolidation tape laying (ISC-ATL) of LM-PAEK carbon fiber-reinforced tapes and the fused filament fabrication (FFF) of neat PEKK to manufacture next-generation multifunctional stiffened panels. A first set of structural planar coupons (500 × 500) were manufactured on quasi-isotropic planar laminates and overprinted gyroid-based stiffeners using a digitally integrated manufacturing cells, gathering key thermal data during the manufacturing of such structures. Manufacturing optimization shows the importance of the thermal history of thermoplastic materials in their crystallization, warping, and interlayer adhesion, both for the ISC panels as well as for the stiffening gyroid elements, for which laser heating systems provide the needed energy density to enhance LM-PAEK

to PEKK adhesion strength by twofold. The first set of stiffened panels were mechanically tested following the flatwise structure standard (ASTM C297 [6]) to characterize the tensile strength of the bonding interface between ISC panels and FFF gyroids, showing values up to 3.1 MPa, as well as the four-point bending test (ASTM D6272-17 [7]) to characterize the flexural strength, achieving 3.554 MPa based on the interlaminar failure of the gyroid layers and a tangent modulus of elasticity of 162 GPa.

2. Experimental Section

The manufacturing of two stiffened panels and the testing conditions are discussed below.

USE CASE 1: The laminate was manufactured with CF/LM PAEK tape, with 16 layers on a quasi-isotropic distribution, following this lay-up sequence: [−45/45/0/0/90/90/45/−45]s. After the skin has been manufactured, the stiffeners were printed on top of the laminate using a PEKK polymer, and for the first layer adhesion, a laser system was used on the head of the robot to solve the problems related with layer adhesion. To increase the stiffness of the overprinted gyroid structure, a layer of continuous CF/PEKK at 0° was printed by FFF. An exemplary video (see Supplementary Information) of the manufacturing of this demo can be found in this link [8].

USE CASE 2: In this configuration, the main difference is the trapezoidal geometry of the stiffener and the top reinforcement. In this case, to increase the stiffness of the stiffener, a top reinforcement was manufactured by ATL, having a total of 8 plies and the following lay-up sequence: [45/−45/0/90/90/0/−45/45].

The result of both prototypes manufactured for this study are shown in Table 1.

Table 1. Stiffened panel designs and main manufacturing parameters.

USE CASE 1	**USE CASE 2**
cuandrangular stiffener	trapezoidal stiffener
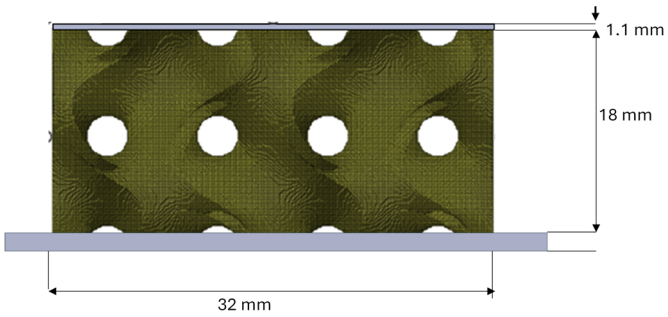	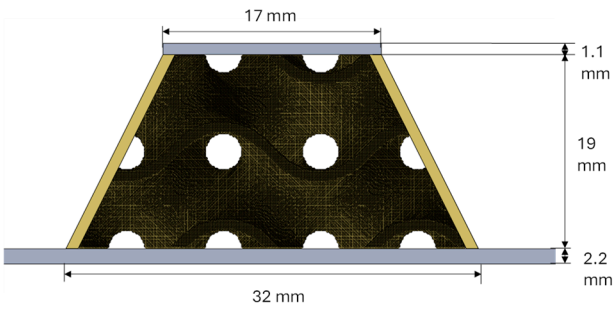

ATL parameters LM-PAEK: Laser-assisted in situ consolidation: speed: 250 mm/s; compression force: 500 N, temperature: 400 °C.
USE CASE 1 and 2: bottom laminates, 16 plies. USE CASE 2: top laminate, 8 plies.
FFF parameters PEKK: Nozzle T[a]: 370 °C; printing speed: 20 mm/s; laser preheating temperature: 350 °C.
FFF parameters CCF-PEKK (Only use case 1): Nozzle T[a]: 390 °C; layer height: 0.4 mm; printing speed: 10 mm/s;
laser power: 7.5 W; laser preheating temperature: 350 °C.

The structural demos presented were mechanically tested, starting with a flatwise test to quantify the adhesion between the ATL laminates and the FFF gyroids, and followed with a four-point bending test of the whole structure.

Flatwise test: The flatwise test was carried out under ASTM C297 [6] over 6 repetitions of 75 × 75 cm coupons to determine the plane tensile strength of the gyroid structure as well as the bond between the gyroid structure and the laminate. Figure 1 shows a schematic of the configuration of the test samples. The specimens were manufactured using ATL to create an in situ consolidated laminate of CF/LM PAEK tape with 16 layers. The layers were arranged in a quasi-isotropic distribution with the following lay-up sequence: [−45/45/0/0/0/0/90/90/90/45/−45]s. On top of this laminate, a full polymer layer was

deposited using FFF technology. Subsequently, a gyroid structure was printed on this polymer layer. To ensure good adhesion of the first printed layer to the laminate, a laser system was mounted on the robot head and used.

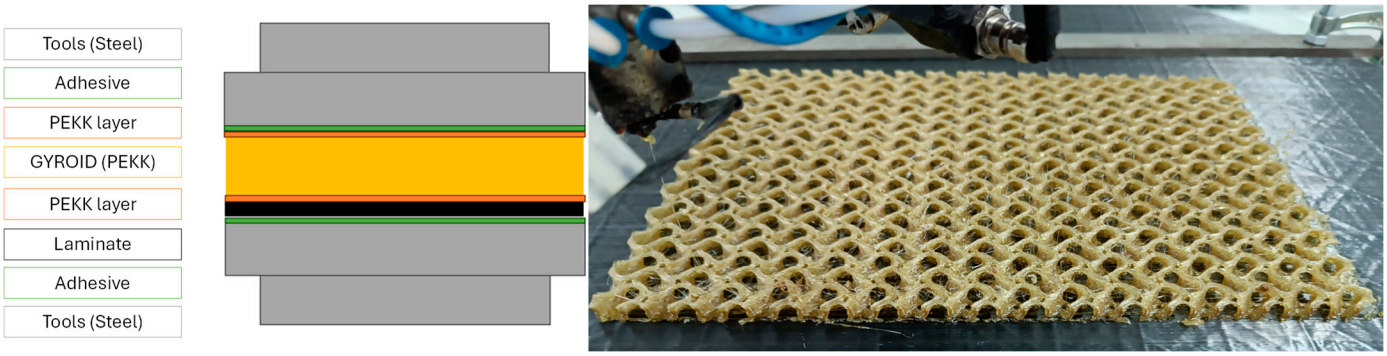

Figure 1. Schematic of flatwise test samples configuration. Flatwise specimen manufacturing process. (Grey = steel too; Green = Adhesive; Orange = PEKK layer; Yellow = gyroid; Black = laminate).

Four-Point Bending Test

All laminates were tested (two repetitions for each use case) according to the ASTM 6272 standard, which outlines the procedures for determining the flexural properties of reinforced plastics. A SHIMADZU 5 kN testing machine (Model No. EENSTC_005, Serial No. 31080, Shimadzu Corporation, Kyoto, Japan) was used. The experimental setup is illustrated in Figure 2. The setup included a support span (L) of 266 mm, a loading nose span of 133 mm, and a support span-to-depth ratio of 120. The supports and loading noses had diameters of 10 mm. The test was conducted at a speed of 1 mm/min until a preload of 5 N was reached, and then this increased to 6.5 mm/min until completion. For this setup, the total thickness of the laminate and stiffeners combined was 21 mm. However, to assess the bending behavior, only the thickness of the laminate, averaging 2.2 mm, was used as the depth of the beam. A key concern with this setup was the non-uniform thickness due to the stiffened elements. To address this, grooves were made in the lower supports to accommodate the gyroids, ensuring that contact was only made with the laminate. This approach aligns with the ASTM 6272 [7] standard for determining flexural behavior.

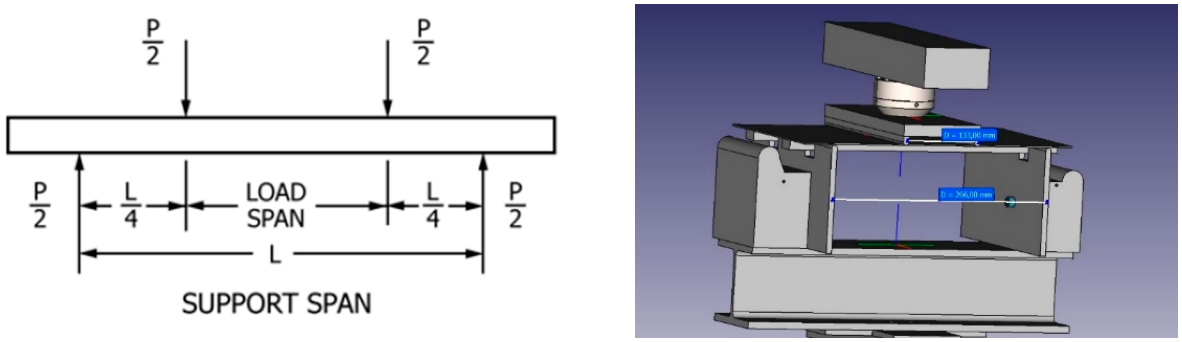

(**a**) (**b**)

Figure 2. Four-point bending configuration. (**a**) Schematic diagram of experiment setup. (**b**) Four-point bending test apparatus.

The tests were monitored using the following equipment: (i) a potentiometer (50 mm, No. UMEM_011, Epromext, Spain) placed on the bottom side of the laminate, 10 mm from the right edge, (ii) an extensometer (Extensometer: 50 mm, No. HMEDEX_011, Epsilon-tech, Jackson, Wyoming, USA) positioned at the center of the bottom side of the laminate,

and (iii) strain gauges placed on both sides of the laminate. The gauges were attached to the laminates using Loctite EA9466 adhesive (Henkel, Düsseldorf, Germany).

The loads applied during the four-point bending test applied to the stiffened laminates tested consisted on the following load sequence:

1. Preload at 5 N/Load up to 700 N/unloading;
2. Preload at 5 N/Load up to 700 N/unloading;
3. Preload at 5 N/Load up to 1000 N/unloading;
4. Preload at 5 N/Load up to 1850 N, then continue up to breakage/unloading;
5. Load up to total breakage.

3. Results

The results obtained during the test of the four stiffened laminates are detailed below.

3.1. Flatwise Test

The six repetitions of the flatwise test resulted in 17.413 ± 1.499 N, which is the equivalent to 10.83 ± 0.93 MPa considering an effective planar area of the gyroid stiffener of about 28.57%. A cohesive failure mode of the stiffener core is observed (Figure 3a), which occurs within the core material itself and indicates that this zone is weaker than the bond between the core and the face sheets. Generally, only cohesive failures are accepted as valid failure modes in flatwise tensile tests. This is because cohesive failure within the core material indicates that the bond between the core and the face sheets is sufficiently strong, and the core material itself is the limiting factor in terms of strength. Cross-sectional micro-tomography was carried out on gyroid structures to analyze porosity distribution, as shown in Figure 3b,c below. As can be observed in the middle and right image, gyroid manufacturing generated a large quantity of porosity between beads. This may be caused by the low temperature deposition not enabling the as-deposited PEKK filament to properly flow. Despite the deposition temperature sufficiently reaching the melting point, the as-extruded material finds a cold substrate (in the range of 110 °C as compared to the extrusion temperature of around 400 °C), which may cause the rapid solidification of the extruded material, thus jeopardizing the proper flow and minimization of porosity.

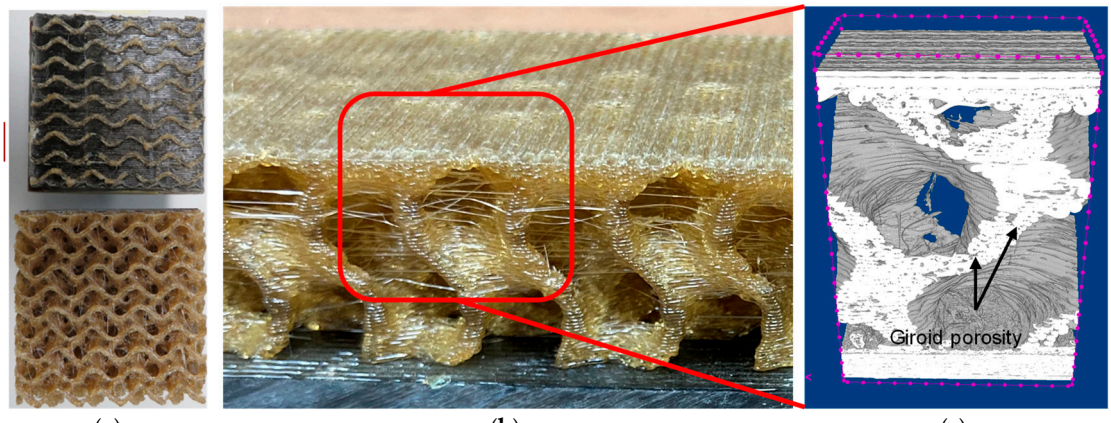

Figure 3. (**a**) Cohesive failure of PEKK gyroid, (**b**) gyroid image, and (**c**) tomography zoom-in indicating porosity between beads in the gyroid, leading to cohesive failure.

3.2. Four-Point Bending Test

Below, we discuss the results obtained during the four-point bending test of the stiffened laminates use cases for each of the load cycles detailed above. Figure 4 shows

the testing results and pictures of the stiffened laminate after being tested, and they are summarized in the Table 2 below.

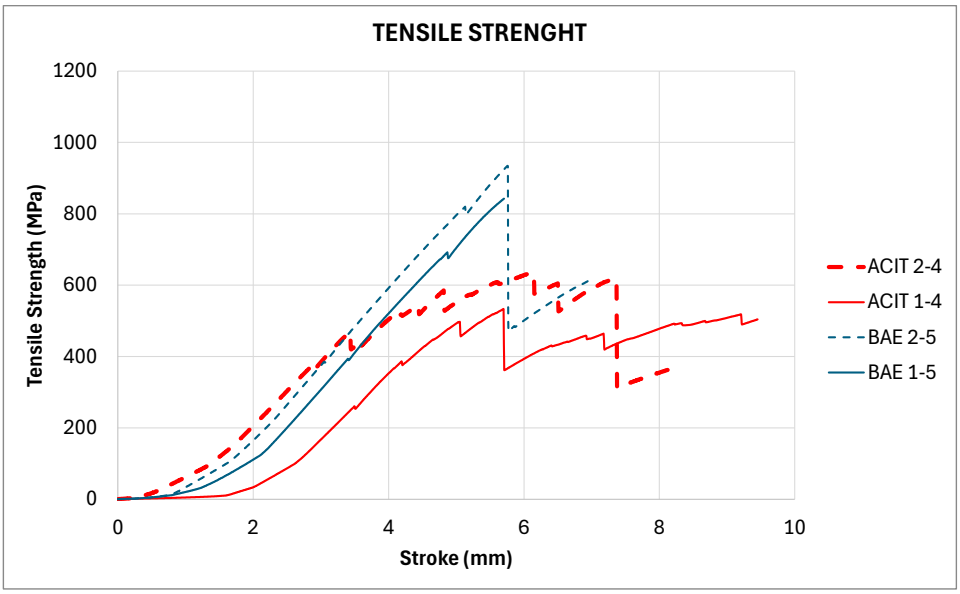

(**a**)

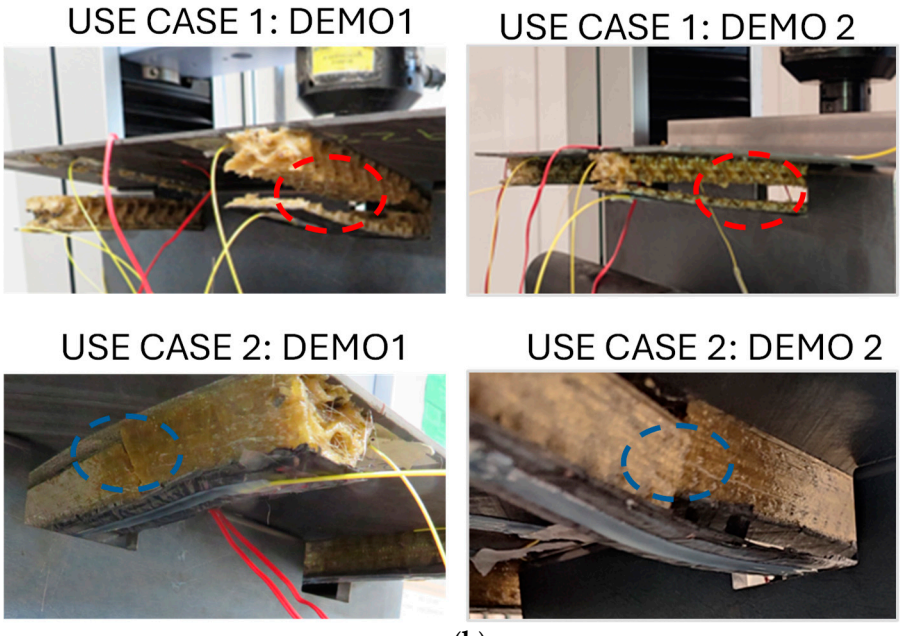

(**b**)

Figure 4. Four-point bending test results. (**a**) Tensile strength versus stroke; (**b**) images of the tested laminates highlighting the different failure modes.

Table 2. Four-point bending test results.

	Maximum Load (N)	Flexural Strength (MPa)	Tangent Modulus of Elasticity (GPa)
U1-D1	3883	533.44	1282
U1-D2	4621	635.03	1257
U1 average	4252 ± 522	584 ± 72	1270 ± 18
U2-D1	6133	842,66	1456
U2-D2	6803	934,65	1476
U2 average	6468 ± 474	889 ± 65	1466 ± 14

Stiffened laminate USE CASE 1-DEMO 1 and 2. In both cases, the failure mode corresponds to the longitudinal failure of the PEKK gyroid stiffener at a height about 75% from the laminate surface in both demos. The carbon fiber laminate and the top CCF reinforcement did not present delamination/failure.

- (U1-D1): At first, some micro failures occur inside the gyroid structures until the first visible failures appear, being cracks in one of the stiffeners at 3600 N of load and 5.1 mm of stroke. The cracks within the gyroid structure continued to grow with the increasing load, achieving a maximum load of 3883 N and 5.6 mm stroke, reaching a flexural strength of 533.44 MPa.
- (U1-D2): The failure mode is similar to that obtained for U1-D1 stiffened laminate's cohesive failure mode at different levels of the gyroid structure. A crack/delamination appeared in the center of one stiffener, between the carbon laminate and PEKK stiffener, and it was propagated along it, generating a delamination in the middle of it. While stiffener 2 did not collapse, the maximum load is similar to that obtained for U1-D1, while the stroke is a little lower. The maximum load achieved was 4621N at 6.3mm of stroke, reaching a maximum flexural strength of 635.03 MPa.

Stiffened laminate USE CASE 2-DEMO 1 and 2. Use case 2 showed a 52% increase in tensile strength as compared to use case 1, leading to a different failure mode based on the cohesive failure of the stiffener very close to the joint of the laminate, leaving behind the PEKK layer consolidated to the ATL laminate with laser.

- (U2-D1): Figure 4 shows the pictures of the stiffened broken laminate at the end of the four-point bending test. In this case, the failure mode is cohesive, since it has failed between the first layer printed with laser against the laminate and the printed stiffener, although the breakage occurred between the printed structures and not at the joint between the FFF and the AFP laminate. When the deformation is sufficiently high, the stiffener fails transversaly, as can be seen in Figure 4. This may be due to the increased stiffness of the gyroid structure, achieved by covering both side walls with a polymer layer. In this case, some cracking sounds began to be heard at 2800 N; at 5000 N, the laminate cracks sound louder and stronger; and at 6200 N, the laminates finally break. The graph in Figure 4 shows that the maximum achieved load of 6133 N occurred at a stroke of 5.8mm, reaching a maximum flexural strength of 842.66 MPa.
- (U2-D2): The stiffener failed by cohesive failure, the same failure mode as that of U2-D1; it failed between the first layer printed with laser against the laminate and the printed stiffener, and the breakage occurred between the printed structures and not at the joint between the FFF and the AFP laminate. In addition, the upper reinforcement by ATL laminate was cohesively separated from the printed part in one of the stiffeners. When the deformation is sufficiently high, the stiffener breaks transversasly. In this case, failure started at 5800 N, although visually, nothing was observed in the stiffened laminate. At 6803 N, stiffener 2 breaks. At this point, the test is paused and unloaded to analyze the laminate status, and then, a final load of up to 5000N if applied when stiffener 1 breaks. As Figure 4 shows, both stiffeners broke in the central–end part of the laminate, and the stiffeners detached from the carbon laminate base in the central area. The graph in Figure 4 shows the maximum value achieved, at 6803 N, which occurred at a stroke of 5.5 mm, reaching a maximum flexural strength of 934.65 MPa.

4. Conclusions

Two use cases (300 × 500 mm) consisting of stiffened laminates, combining the laser-assisted in situ consolidation of LMPAEK tapes by automated tape laying and the over-printing of PEKK gyroids by FFF, were successfully manufactured, demonstrating the

feasibility of using the combination of laser-assisted in situ consolidation ATL and FFF for high-performance thermoplastics (LMPAEK and PEKK), leading to intermediate-to-high mechanical properties of up to 889 MPa on four-point bending tests. Despite the good adhesion between overprinted PEKK gyroids and LMPAEK laminates assisted by laser, based on tomography analysis and the flatwise mechanical results, it has been shown that there is still room for process optimization from the temperature point of view to minimize internal porosity and enhance interlaminar adhesion. From the design point of view, improvements of the mechanical properties have been demonstrated by shifting to trapezoidal stiffeners with closed external walls and quasi-isotropic top reinforcement, as compared to quadrangular stiffeners and unidirectional continuous carbon fiber-reinforced layers. Future work concerning product temperature management (nozzle-optimized design, embedded local heating on the nozzle, or heated table) and demonstrations should be carried out.

Supplementary Materials: The following supporting information can be downloaded at https://www.youtube.com/watch?v=9usi16RtsSY (accessed on 20 May 2024).

Author Contributions: Conceptualization, P.R.-R., methodology, P.R.-R., A.R. and B.S.-P., software, A.R. and B.S.-P., validation, N.G.-C., A.P. and P.R.-R., formal analysis, N.G.-C., investigation, A.R. and B.S.-P., resources, P.R.-R., data curation, N.G.-C., B.S.-P., A.P. and P.R.-R., writing—original draft preparation, N.G.-C. and A.P.; visualization, N.G.-C., A.P. and P.R.-R., supervision, P.R.-R., project administration P.R.-R., funding acquisition, P.R.-R. All authors have read and agreed to the published version of the manuscript.

Funding: This research was funded by European Commission H2020 Program, DOMMINIO Project Grant Number GA101007022.

Institutional Review Board Statement: Not applicable.

Informed Consent Statement: Not applicable.

Data Availability Statement: https://dominioproject.eu/, https://cordis.europa.eu/project/id/101007022 (accessed on 20 May 2024).

Acknowledgments: Acknowledge support from Silvia Trillo for mechanical Testing and Elena Rodríguez-Senin, Fernando Sanchez and Alberto Fernandez for project conceptualization.

Conflicts of Interest: The authors declare no conflicts of interest.

References

1. Das, A.; Chatham, C.A.; Fallon, J.J.; Zawaski, C.E.; Gilmer, E.L.; Williams, C.B.; Bortner, M.J. Current understanding and challenges in high temperature additive manufacturing of engineering thermoplastic polymers. *Addit. Manuf.* **2020**, *34*, 101218. [CrossRef]
2. Gkartzou, E.; Zafeiris, K.; Tsirogiannis, C.; Pedreira, A.; Rodríguez, A.; Romero-Rodriguez, P.; Gakis, G.P.; Kosanovic-Milickovic, T.; Kyritsis, A.; Charitidis, C.A. Induction Heating of Laminated Composite Structures with Magnetically Responsive Nanocomposite Interlayers for Debonding-on-Demand Applications. *Polymers* **2024**, *16*, 2760. [CrossRef] [PubMed]
3. Zarzoso, M.; Mikhalchan, A.; Mocerino, D.; Romero-Rodriguez, P.; Losada, R.; Vilatela, J.J.; González, C. Strain sensing of structural composites by integrated piezoresistive CNT yarn sensors. *Compos. Part B Eng.* **2024**, *286*, 111752. [CrossRef]
4. Najmon, J.C.; Raeisi, S.; Tovar, A. Review of additive manufacturing technologies and applications in the aerospace industry. *Addit. Manuf. Aerosp. Ind.* **2019**, 7–31.
5. García-Dominguez, A.; Claver, J.; Sebastián, M.A. Integration of Additive Manufacturing, Parametric Design, and Optimization of Parts Obtained by Fused Deposition Modeling (FDM). A Methodological Approach. *Polymers* **2020**, *12*, 1993. [CrossRef] [PubMed]
6. *ASTM C297-94(1999)*; Standard Test Method for Flatwise Tensile Strength of Sandwich Constructions. ASTM: West Conshohocken, PA, USA, 1999.

7. *ASTM D6272-17*; Standard Test Method for Flexural Properties of Unreinforced and Reinforced Plastics and Electrical Insulating Materials by Four-Point Bending. ASTM: West Conshohocken, PA, USA, 2020.
8. DOMMINIO Project | Multi-Stage Manufacturing Combining ATL and 3D Printing Processes. Available online: https://www.youtube.com/watch?v=9usi16RtsSY (accessed on 20 May 2024).